RUBIDIUM VAPOR CELL WITH INTEGRATED NONMETALLIC MULTILAYER REFLECTORS

M.A. Perez[1], U. Nguyen[2], S. Knappe[3], E. Donley[3], J. Kitching[3] and A.M. Shkel[1]
[1]MicroSystems Labratory, University of California, Irvine, CA, USA
[2]Electrical Engineering and Computer Science, University of California, Berkeley, CA, USA
[3]Time and Frequency Division, National Institute of Standards and Technology, Boulder, CO, USA

ABSTRACT

This paper reports on a method for improving the optical efficiency of micromachined reflectors integrated in rubidium vapor cells. A hybrid bulk micromachining and multilayer thin film process is used to form the reflectors on angled sidewalls, which redirect laser light through the vapor cell and back toward the plane of the source with reduced optical power loss. The optical return efficiency of two paired dielectric reflectors is shown to be improved by as much as eight times over silicon reflectors alone. The D_1 absorption line in a one cubic millimeter miniature alkali ^{87}Rb vapor cell by use of two integrated thin film reflectors is experimentally demonstrated.

1. INTRODUCTION

The engineering of miniature vapor cells for the encapsulation of gases is of widening interest. Such cells form the central elements in emerging MEMS technologies based on the atomic transitions of alkali gases, such as miniaturized atomic clocks and magnetometers [1], [2]. Micromachined vapor cells have been previously proposed and demonstrated by use of a variety of innovative techniques, including wafer level glass blowing [3].

In many vapor cell applications, integrated optical reflectors are required for optical routing through the cell. Such designs are preferable for system integration and miniaturization, because the light is returned to the plane of the source. This allows the optical source and detection elements to be located on the same side of the cell. For example, the Honeywell [4] Chip Scale Atomic Clock (CSAC) incorporates micromachined angled silicon reflectors within a rubidium vapor cell for routing laser light through the cell from a Vertical Cavity Surface Emitting Laser (VCSEL) to a coplaner photodiode [5]. Even though simpler to implement, bare silicon is not expected to perform as efficiently as an optical reflector, yielding optical losses that may limit device performance.

Other devices incorporate deposited optical films to improve the reflective efficiency. A simple reflector may be formed by incorporating a metallic film, such as a copper reflector used in the vapor cell of the Symmetricom [4] CSAC [6]. Due to effects such as thermal currents, metallic reflectors within the vapor cell may disturb the sensitive electromagnetic environment required for many miniature vapor cell applications [7]. In contrast, thin film dielectric structures may be used to improve the reflector efficiency without metals.

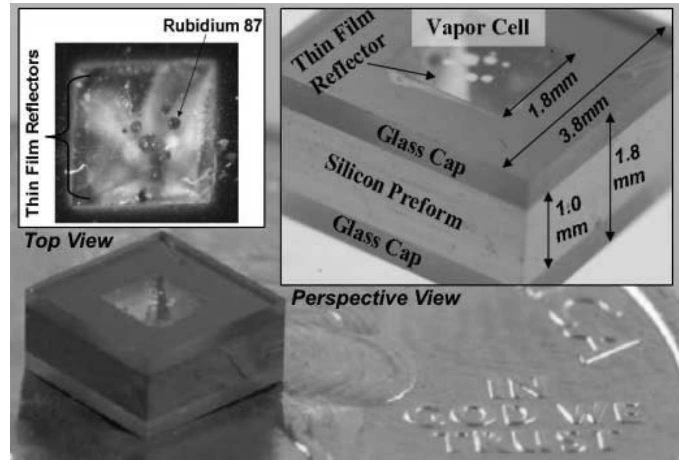

Fig. 1. *Vapor cell with integrated multilayer thin film reflectors (on a US quarter for scale) with dimensioned perspective and top view inserts*

This paper demonstrates a set of high efficiency nonmetallic multilayer thin film reflectors integrated into a micromachined rubidium vapor cell, shown in Figure 1.

2. DESIGN

Silicon Reflectors

Chemically etched angled silicon surfaces have long been reported to be applicable for redirecting optical beams (for example, see [8]). However, the reflective properties of an uncoated, bare silicon surface is expected to be poorly suited for the high-efficiency routing of light, as may be required for micro-scale atomic devices such as described in [9]. The maximum reflection of general, unpolarized light from an ideal silicon surface may be calculated from the optical properties of bulk silicon. At an optical wavelength λ of 795 nm, the complex optical index of silicon is $n+ki = 3.68+7*10^{-3}i$, where n is the index of refraction and k is the coefficient of extinction of the material. The reflectivity from the surface of a bulk material may be calculated as

$$R = \frac{(n-1)^2+k^2}{(n+1)^2+k^2}, \quad (1)$$

which for silicon yields a reflectivity of 0.33 [10]. This indicates that a maximum of 33 % of the optical energy will be reflected from a silicon surface, with the remaining energy transmitted through the reflector material. For the reflection from two silicon surfaces, such as is required for return reflection, $R_{total} = R^2 = 0.11$. This indicates a loss of at

least $1 - R_{total} = 0.89 = 89$ % from transmission through a bare silicon return reflector cell, which is undesirable.

Dielectric Multilayer Reflectors

Multilayer structures of thin films of dielectric material may be used to increase the optical efficiency of the reflector cell. In the Distributed Bragg Reflector (DBR), light reflected at the interface between each layer is designed to constructively interfere to maximize the total reflected optical power at a specific wavelength. The reflectivity is maximized if the structure is composed of alternating layers of two materials of different indices of refractions, and if the optical thickness of each layer is one-quarter wavelength of the light to be reflected, such that

$$t_{layer} = \frac{\lambda}{4n}, \tag{2}$$

where t_{layer} is the thickness of each layer, λ is the wavelength of light to be reflected and n is the index of refraction of each layer. The reflectance of such a structure at λ is given by

$$R = \left(\frac{1 - \left(\frac{n_H}{n_L}\right)^{2p} \left(\frac{n_H^2}{n_s}\right)}{1 + \left(\frac{n_H}{n_L}\right)^{2p} \left(\frac{n_H^2}{n_s}\right)} \right)^2, \tag{3}$$

where n_H and n_L are the higher and lower index of refractions of each of the thin film materials, respectively, p is the number of layer pairs, and n_s is the index of refraction of the substrate [11]. The materials are assumed to be optically lossless ($k = 0$). It can be readily seen that reflectivity increases rapidly for both an increasing optical index contrast ($\frac{n_H}{n_L}$) and for an increasing number of layers.

A variety of dielectric materials are available for deposition onto silicon structures using conventional thin film techniques. Amorphous silicon (αSi) provides a high index of refraction at $n_H = 3.9$, while silicon dioxide (SiO_2) has a low index at $n_L = 1.45$ at $\lambda = 795$ nm [10]. Use of these materials yields a high optical index contrast ($\frac{n_H}{n_L} = 2.7$). On a silicon substrate, $p = 3$ layer pairs (six total layers) forms a mirror of $R = 0.997$, or better than 99 % efficiency after two reflections.

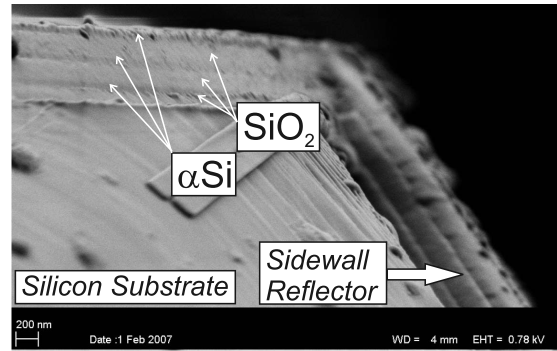

Fig. 3. *Cross section of a 6-layer (alternating 60 nm αSi (darker), 140 nm SiO_2 (lighter)) quarter wave multilayer thin film reflector onto the top surface and angled sidewall of anisotropically etched silicon for use as a vapor cell preform*

3. FABRICATION

The fabrication of the cell is a hybrid of traditional bulk micromachining [12], optical thin film deposition [13], and anodic wafer bonding [14]. Referring to Figure 2, the first three steps are a traditional silicon wet through-etch. The next four steps are the processing related to the optical films. The final step is the encapsulation of alkali vapor and buffer gasses.

In Step 1, we start with a 1 mm thick double side polished (DSP) undoped silicon wafer. On each side of the wafer, a 3000 Å thick silicon nitride layer is deposited via Low Pressure Chemical Vapor Deposition (LPCVD). The silicon nitride is used as a wet etch hardmask. In Step 2, a 1.8 mm sided square is patterned lithographically using a AZ4620 photoresist mask. This mask is aligned to the <100> wafer flat. The cell window pattern is transferred to the silicon nitride hardmask via a short Reactive Ion Etch (RIE). In Step 3, the patterned wafer is immersed in a bath of 45 % (by volume with water) potassium hydroxide (KOH) to which is

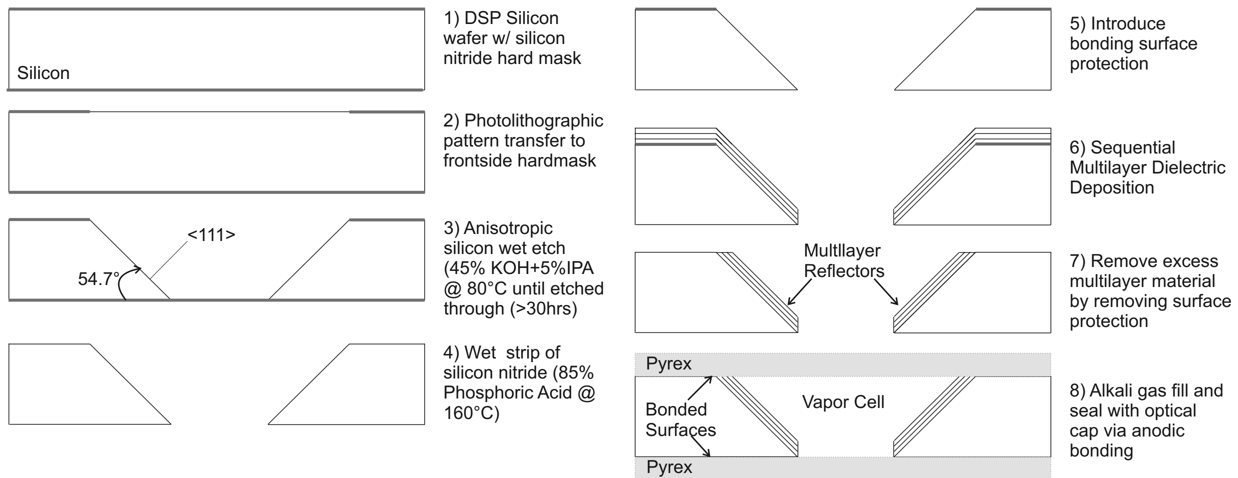

Fig. 2. *Fabrication of the bulk micromachined silicon reflector preform with the high reflectance multilayer sidewall reflector, including the final anodic bonding and gas encapsulation process.*

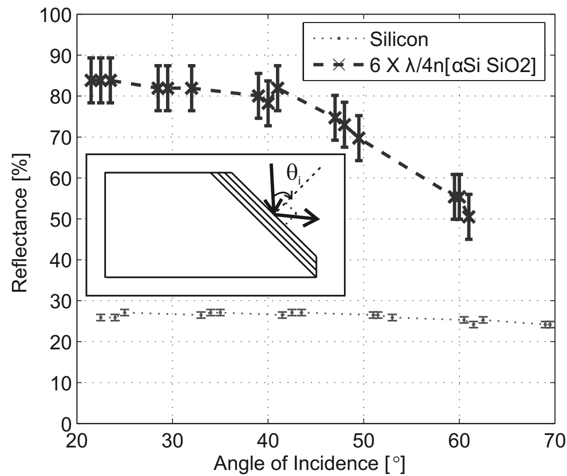

Fig. 4. *Reflectance from a single bulk micromachined silicon sidewall reflector with and without multilayer reflectors*

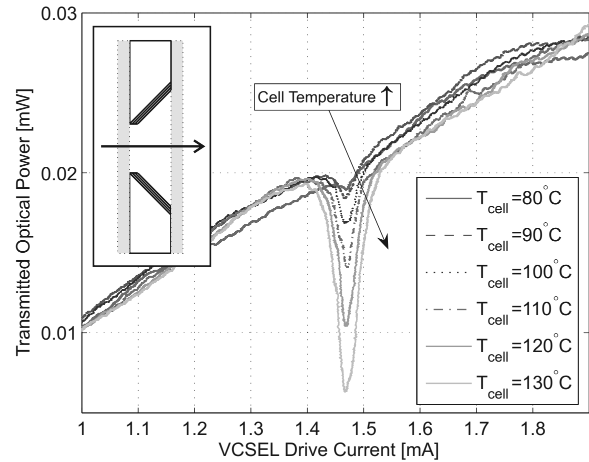

Fig. 5. *Optical absorption in the vapor cell under elevated temperature (T_{cell}) under swept emission from a VCSEL through due to the ^{87}Rb D_1 atomic transition*

added 5 % (by volume) isopropanol alcohol (IPA). The bath is heated to $80\ ^{\circ}C$, causing the exposed silicon to etch at ~ 0.5 $\mu m/min$ revealing the surfaces of the <111> crystalline planes. This forms a cell with flat, angled sidewalls inclined at $54.7°$ to the wafer surface. The etch is allowed to progress through the wafer, typically taking more than 30 hours.

In Step 4, the silicon nitride hardmask is chemically removed via a hot $160\ ^{\circ}C$ phosphoric acid dip. In Step 5, the top surface of the etched silicon is stamped onto a shallow photoresist film and allowed to dry, which provides protection to the anodic bonding surfaces during subsequent deposition. Then in Step 6, the optical films are sequentially deposited by plasma enhanced chemical vapor deposition (PECVD) via a PlasmaTherm 790. A cross section of a structure after Step 6 is shown in Figure 3. In Step 7, the final cell preform is fabricated by removing the top surface protection via a fuming sulfuric acid dip, resulting in the lift-off of the excess thin film material and cleaning of the surfaces.

In Step 8, the preform is filled with the alkali material, as has been previously described in [2]. In brief, the filling method consists of combining BaN_6 and $^{87}RbCl$ inside a glass ampoule. The ampoule nozzle is aligned to the cell preform within a vacuum chamber and heated to release ^{87}Rb into the cell preform. Then buffer gases are released into the chamber and the cell is sealed via anodic bonding between two Pyrex 7740 plates. In this case, the vapor cell was filled with ^{87}Rb along with 153 Torr Xe and 1100 Torr N_2 buffer gases. The top Pyrex plate allows optical access to the vapor.

4. RESULTS

To characterize the reflection of an individual etched sidewall, a cell after Step 7 of fabrication was split and mounted on a rotation stage. In the experiment we used a single mode VCSEL from ULM [4] temperature stabilized at $20\ ^{\circ}C$ [15]. The collimated light beam from the VCSEL was directed at the surface. The reflected beam was collected and the power was monitored by a photocollector at different reflection angles of incidence. The power collected is normalized by the VCSEL emission power, as shown in Figure 4. The reflective surfaces of the cell are characterized to have a reflectance over 80 % for incident angles up to $40°$, which is almost three times greater than that of identically etched bare silicon sidewall reflector, which exhibits a reflectance under 30 %.

To characterize the optical absorption by the encapsulated vapor, the light from the VCSEL was passed directly through the complete vapor cell, shown in Figure 1. A small resistive heater was used to elevate the cell temperature, increasing the vapor pressure of the ^{87}Rb within the enclosed cell. The emission wavelength of the VCSEL was swept by varying the drive current at constant VCSEL temperature from approximately 794.5 nm at 1.0 mA to 795.1 nm at 2.0 mA. At increased vapor pressure under elevated temperatures, wavelength swept VCSEL light transmitted through the cell showed significant absorption at the D_1 atomic transition of ^{87}Rb (794.8 nm in air), demonstrating alkali vapor encapsulation (Figure 5).

The VCSEL beam was then directed onto one sidewall of the cell. The beam was reflected through the cell and redirected back towards the plane of emission by the reflector on the opposite sidewall, where the optical power is collected and monitored. The temperature of the cell was held fixed at a temperature of $100\ ^{\circ}C$ using feedback control and the VCSEL drive current is tuned until a pronounced absorption peak is detected indicating vapor cell interrogation under retro-reflected light (Figure 6). When normalized by the optical power of the source, under this retro-reflective path, an optical efficiency of 40 % for the reflector cell was demonstrated. This is four times better than the 10 % retro-reflection efficiency from a similarly etched silicon cell preform.

Not included in the efficiency of the bare silicon preform are losses due to the cap window and scattering from condensed rubidium. These are additional to reflector inefficiencies in the complete vapor cell. An optical efficiency approaching 80 % was observed in a preform incorporating thin film reflectors fabricated along side the complete vapor cell. Comparing this preform and the vapor cell indicates that the multilayer reflectors improve the optical efficiency by a

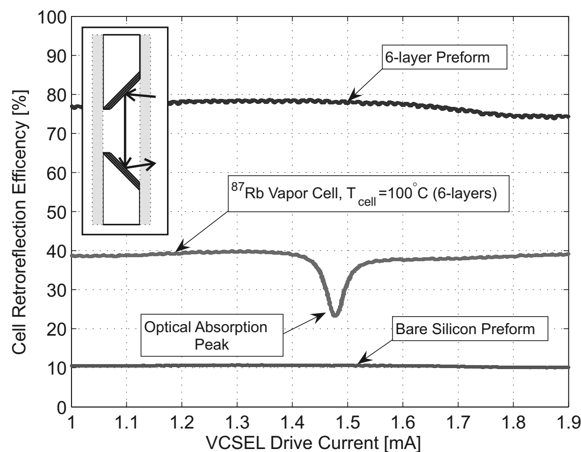

Fig. 6. *Optical efficiency of the vapor cell and cell preforms during return reflection with and without integrated reflectors*

factor of eight for an optical path with two reflections.

5. DISCUSSION

Although the optical performance of the cell was increased dramatically over that expected from a vapor cell formed from uncoated silicon, the performance was less than might be expected from the analytical estimates according to equation (3). This is most likely due to the variations in the thin film thickness from the optical optimum thickness expressed by equation (2). A color gradient is clearly evident to the naked eye, as in the top view insert in figure 1. This gradient progresses along the sidewall reflector from the top of the vapor cell to the bottom and shows a shift from red to blue. This indicates a shift in the wavelength λ at which the mirror has maximum reflectance from the longer red wavelengths at the top of the cell, for which the mirror was designed and at which it was tested, to lower blue wavelengths of maximum reflectance at the bottom of the cell. This is likely due to a nonuniform deposition rate, which decreases as deposition on surfaces progresses downward into the cell. At the design and test wavelength of $\lambda = 795\ nm$, this variation necessarily reduces the reflectance over that estimated from equation (3). In addition, this nonuniformity currently prevents the implementation of more advanced thin film designs with added functionality, such as phase shifting reflectors [16]. Such advanced designs may be implementable under fabrication conditions optimized for sidewall film uniformity.

6. CONCLUSIONS

This paper demonstrates the use of multilayer thin film structures deposited on bulk micromachined surfaces for integrated reflectors in atomic vapor cells. In spite of process imperfections due to nonuniform deposition on angled surfaces, it is shown experimentally that the multilayer reflectance is almost three times better than that of bare silicon. When used for a reflective path requiring two reflections within a micromachined cell, the optical efficiency may be improved by as much as eight times. A process suitable for the fabrication of encapsulated rubidium vapor cells from such cells with integrated multilayer reflectors is demonstrated.

ACKNOWLEDGMENT

The authors thank the staff of the Integrated Nanosystems Research Facility (INRF) for fabrication support and A. Schofield for micrograph assistance. This work was supported in part by the Defense Advanced Research Projects Agency (DARPA) Navigation-Grade Integrated Micro Gyroscopes (NGIMG) program and is a partial contribution of the National Institute of Standards and Technology (NIST), an agency of the US government, and is not subject to copyright.

REFERENCES

[1] L.-A. Liew, S. Knappe, J. Moreland, H. Robinson, L. Hollberg, and J. Kitching, “Microfabricated alkali atom vapor cells,” *Appl. Phys. Lett.*, vol. 84, p. 2694, 2004.
[2] S. Knappe, V. Gerginov, P. D. D. Schwindt, V. Shah, H. G. Robinson, L. Hollberg, and J. Kitching, “Atomic vapor cells for chip-scale atomic clocks with improved long-term frequency stability,” *Opt. Lett.*, vol. 30, pp. 351, 2005.
[3] E. Eklund, A. Shkel, S. Knappe, E. Donley, and J. Kitching, “Spherical rubidium vapor cells fabricated by micro glass blowing,” in *Proc. 20th IEEE Int. Conf. Micro Electro Mechanical Systems*, 2007, pp. 171.
[4] “Products or companies named here are cited only in the interested of complete scientific description, and neither constitute nor imply endorsement by NIST or by the US government.”
[5] D. Younger, L. Lust, D. Carlson, S. Lu, L. Forner, H. Chanhvongsak, and T. Stark, “A manufacturable chip-scale atomic clock,” in *Transducers ’07 & Eurosensors XXI: The 14th Int. Conf. on Solid-State Sensors and Actuators and Microsystems*, June 2007.
[6] R. Lutwak, J. Deng, W. Riley, M. Varghese, J. Leblanc, G. Tepolt, M. Mescher, D. K. Serkland, K. M. Geib, and G. M. Peake, “The chip-scale atomic clock low-power physics package,” in *36th Annual PTTI Systems and Applications Meeting Proc.*, 2004.
[7] E. A. Donley, E. Hodby, L. Hollberg, and J. Kitching, “Demonstration of high-performance compact magnetic shields for chip-scale atomic devices,” *Review of Scientific Instruments*, vol. 78, no. 8, p. 083102, 2007.
[8] D. J. Sadler, M. J. Garter, C. H. Ahn, S. Koh, and A. L. Cook, “Optical reflectivity of micromachined 111-oriented silicon mirrors for optical input - output couplers,” *Journal of Micromechanics and Microengineering*, vol. 7, p. 263, December 1997.
[9] J. Kitching, E. Donley, E. Hodby, A. M. Shkel, and E. J. Eklund, “Compact atomic magnetometer and gyroscope based on a diverging laser beam (2008-002),” UC Irvine Office of Technology Alliances, 2007.
[10] E. D. Palik, *Handbook of Optical Constants of Solids*, E. D. Palik, Ed. Elsevier, 1998, vol. 1.
[11] H. A. Macleod, *Thin-Film Optical Filters*, 3rd ed. IoP, Bristol–Philadelphia, 2001.
[12] G. Kovacs, N. Maluf, and K. Petersen, “Bulk micromachining of silicon,” *Proc. IEEE*, vol. 86, no. 8, pp. 1536, August 1998.
[13] L. Martinu and D. Poitras, “Plasma deposition of optical films and coatings: A review,” *Journal of Vacuum Science & Technology A: Vacuum, Surfaces, and Films*, vol. 18, no. 6, pp. 2619, 2000.
[14] M. Schmidt, “Wafer-to-wafer bonding for microstructure formation,” *Proc. IEEE*, vol. 86, no. 8, pp. 1575, 1998.
[15] ULM Photonics, “Specification for single mode VCSEL 795 ± 3 nm TO46 & TEC,” ULM Photonics
[16] W. H. Southwell, “Multilayer coating design achieving a broadband 90 degree phase shift,” *Appl. Opt.*, vol. 19, p. 2688, 1980.